Impact-formed complex diamond-graphite nanostructures

PÉTER NÉMETH[1]* (ID), KIT MCCOLL[2],
LAURENCE A.J. GARVIE[3], FURIO CORÀ[4],
CHRISTOPH G. SALZMANN[4] and PAUL F. MCMILLAN[4]

[1] Institute for Geological and Geochemical Research, Research Centre for Astronomy and Earth Sciences, Eötvös Loránd Research Network, Budaörsi út 45, Budapest, Hungary

[2] Department of Chemistry, University of Bath, Bath, UK

[3] Buseck Center for Meteorite Studies, Arizona State University, Tempe, AZ 85287, USA

[4] Department of Chemistry, University College London, 20 Gordon Street, London, UK

ABSTRACT

Shock waves resulting from asteroidal and laboratory impacts convert sp^2-bonded graphitic material to sp^3-bonded diamond. Depending on the shock pressure and temperature conditions, complex nanostructures can form that are neither graphite nor diamond but belong to the diaphite material group, which are characterized by structurally intergrown layered sp^2- and sp^3-bonded carbon domains. Our ultrahigh-resolution transmission electron microscopy images combined with density functional theory calculations demonstrate that diaphites have two related but distinct structural families. Here, we describe diaphite nanostructures from natural and laboratory shocked samples, provide a framework for classifying the members of these materials, and draw attention to their excellent mechanical and electronic material properties.

AKJournals

INTRODUCTION

Asteroidal and laboratory impacts generate hypervelocity shock waves that are characterized by an abrupt, nearly discontinuous change in pressure, temperature and density of the medium. This abrupt pressure and temperature changes give rise to non-equilibrium conditions and the formation of novel structures [1, 2]. Of particular interest are impact diamonds (Fig. 1) and diamond-like nanostructures that form during the shock compression of graphitic materials.

Diamond has a cubic structure based on stacked layers of tetrahedrally bonded carbon. However, the impact diamonds tend to exhibit hexagonal features in their X-ray diffraction patterns, which has been used to suggest formation of the alternative "lonsdaleite" structure that has carbon layers stacked in a hexagonal fashion [3]. Recent high-resolution transmission electron microscopy (HRTEM) and X-ray diffraction analyses suggest that pure lonsdaleite has not been identified yet and that the impact-formed diamonds in fact contain intergrown layers of cubic and hexagonal stackings [4–7]. However, these analyses assume that the formed structures contain only sp^3-bonded carbon atoms. Introducing sp^2-bonding into the dominantly sp^3-bonded structure introduces additional features into the TEM images and diffraction patterns of impact diamonds. A composite nanostructure containing crystallographically oriented few-layered graphite domains within sp^3-bonded slabs of diamond has been reported from the extraterrestrially shocked Gujba meteorite [1]. Amorphous
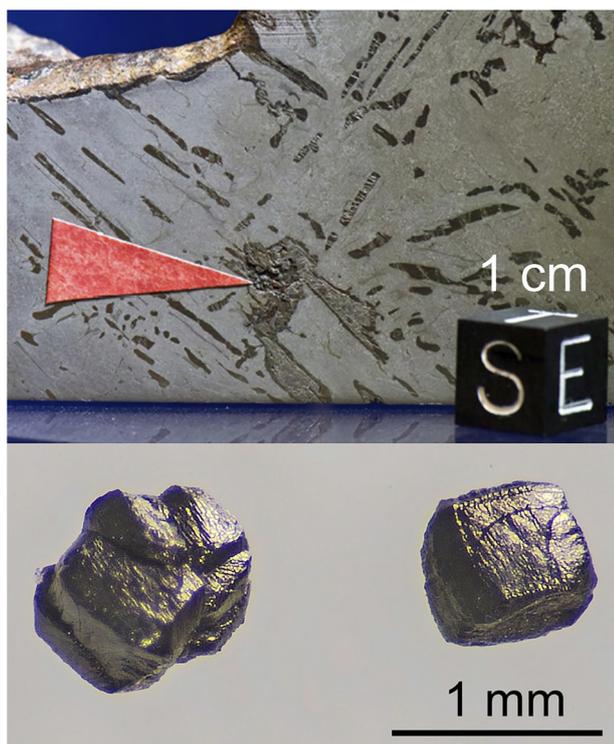
Fig. 1. Impact diamonds from Canyon Diablo iron meteorite (ASU meteorite collection). Red arrow points to the locality of the diamond grains inside kamacite (α Fe/Ni alloy)

carbons containing both sp^2- and sp^3- bonded carbon, and diamond-like carbons (DLCs) exhibiting a high degree of tetrahedral bonding within an sp^2-bonded matrix are synthesized for material science applications [8]. In addition to these amorphous carbon forms, a 2D diamond-graphene nanostructure termed "diaphite" has been proposed to form following photoexcitation of graphite [9].

Here, we present HRTEM images of impact diamonds and demonstrate that these samples contain abundant regions of intimately intergrown graphite and diamond, i.e., diaphite structures. Although the proper distinction between graphite and graphene requires Raman investigation [10], in this paper we associate the TEM findings and the calculation results of 1–5 graphitic layers with graphene and use the word graphite if more than 5 layers are considered. HRTEM analyses reveals that portions of the samples consist of two orientationally dependent interlayered diamond and graphene components, corresponding to the two diaphite types [11, 12]. Using density functional theory (DFT) calculations we identify the structure of these regions and show that diaphites exist at relatively low energy and are competitive with graphite and diamond, and they are expected to be kinetically stable.

EXPERIMENTAL DETAILS

For TEM investigation, samples from Gujba and Canyon Diablo meteorites and the Popigai impact crater were prepared using the protocol described in refs [1] and [4]. Millimeter-sized pieces of black areas were separated from the Gujba meteorite. These were treated with HCl for two days and were washed in distilled water for several times. Distilled water was added to the final carbon residue and ~2 µL droplets of the suspension was dried on a Cu TEM grid coated with lacy-C. 0.5–1 mm-sized euhedral diamond grains were selected from the Canyon Diablo meteorite (Fig. 1) and from the Popigai sample. The grains were crushed between two WC cubes. A droplet (ca. 2 µL) of methanol were added to these crushed grains and these solutions were dried on Lacey-C copper grids.

Bright-field TEM (BFTEM) and HRTEM images were acquired using a JEOL JEM 4000EX electron microscope (400 kV; LaB$_6$ filament, top-entry, double-tilt stage; C_s = 1 mm; point resolution = 0.17 nm). The HRTEM image shown in Fig. 4a was obtained at close to Scherzer defocus (~−40 nm). BF and high angle annular dark-field (HAADF) scanning TEM (STEM) images were obtained with a JEOL ARM200F electron microscope (200 keV, 0.08-nm point resolution) equipped with a CEOS CESCOR hexapole aberration corrector. The HAADF and BF STEM images were recorded for 8 s and obtained with a camera length of 10 cm and the collection angle of 80 and 11 mrad, respectively. STEM images were acquired with spot size 6. Figs 3 and 4a were recorded with the JEOL JEM 4000EX and Figs 2, 4c, 5a and b were acquired with the JEOL ARM200F electron microscope.

Fast Fourier transforms (FFT) were calculated using the Gatan Digital Micrograph 3.6.1 software. The background-filtered image of Fig. 2 was calculated by applying a 0.06-nm−1-size Lorentzian mask filter for the 111 diamond reflections. The approximately same size Lorentzian mask filters were used for the *00l* graphite and *111* diamond reflections to generate Figs 4d, 5a and b. For HRTEM image simulation we used simulaTEM software based on the DFT-generated structure of Fig. 5c applying the following parameters: voltage 200 keV, defocus −405.46 Å, spherical aberration 0.01 mm and defocus spread 38 Å, azimuth angle 30°. The beam spread and astigmatism amplitude values were idealized and set to 0 mrad and 0 Å, respectively. The DFT methods and details of calculated structures are reported in ref. [11].

RESULTS AND DISCUSSION

Ultrahigh-resolution TEM images of diamond

Understanding the nanoscale structural details within diamond requires resolving interatomic spacings less than 0.13 nm, which is only possible with the ultra-high resolution provided by aberration-corrected microscopes. In a conventional (non-aberration corrected) high-resolution electron microscope, only the 0.21 nm set of {111} diamond fringes are visible. However, using aberration-corrected electron microscopes we can also resolve the 0.126 and 0.109 nm spacings corresponding to {220} and {113}
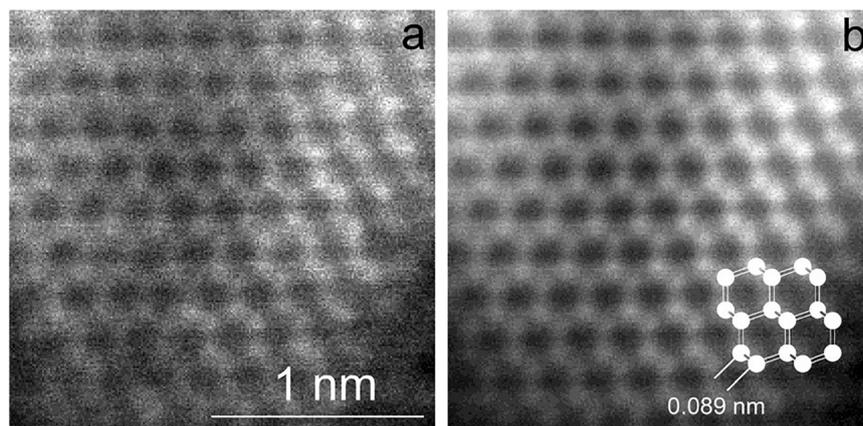
Fig. 2. Atomic resolution TEM image of an impact diamond crystal from Popigai crater. a) Carbon atoms occur as white dots on the raw HAADF STEM image. b) Fourier-filtered image enhances the visibility of the individual atomic columns and shows that the resolution of the image is better than 0.1 nm
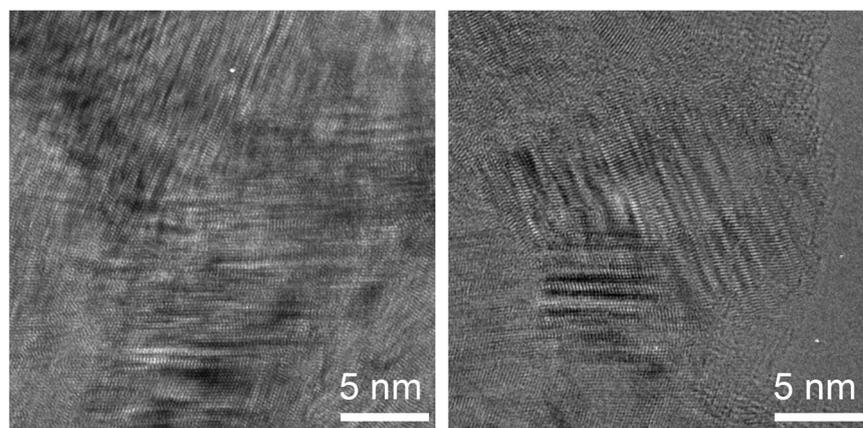

Fig. 3. Low-magnification TEM images from fragments of the Canyon Diablo sample showing structural complexity at the nanoscale (original images reported in [12], copyright Springer Nature Ltd.)

diamond fringes. Furthermore, the improved lens systems of these microscopes even permit the identification of the individual carbon atomic columns (Fig. 2). In the following we will use the term "uHRTEM images" for referring to images that display the 0.126 nm and 0.109 spacings of diamond to distinguish from conventional HRTEM images that can show the 0.21 nm spacings of diamond only.

Type 1 diaphite

BFTEM and HRTEM images of samples from the Gujba and Canyon Diablo meteorite, the Popigai impact crater, and laboratory-shocked graphite reveal the intrinsic structural complexity of the crystalline carbon phases (Figs 3–5) [11, 12]. Of particular interest are nanostructures that exhibit lattice fringe spacings of 0.34 nm (corresponding to the interlayer spacings of graphite) and 0.21 nm, consistent with both *100* graphite and *111* diamond reflections (Fig. 4). Similar structures have previously been attributed to independent graphite, lonsdaleite and diamond present within the samples [3, 13]. However, the 0.34 nm fringes occur systematically as few-layered graphene to graphitic domains and

contiguous with the {111} diamond layers. Their lateral extent varies up to a few nanometers, and they terminate within the sp^3-bonded lattice: we refer to this as Type 1 diaphite.

Since a TEM image shows a 2D projection of superimposed nanodomains, the structure of Type 1 diaphite is most clear in thin (thinner than 20 nm) samples. In thicker (than 20 nm) samples the graphene and {111} diamond fringes are more difficult to recognize, but their contributions can be detected in FFT of the HRTEM data (Fig. 4c). An interesting example is the laboratory shocked graphite, where the superpositions of the nanodomains give rise to a complex cross-fringe pattern [11].

Type 2 diaphite

The investigation of impact diamond samples using aberration-corrected TEMs reveal hexagonally arranged graphitic carbon layers inserted within and bonded at high angles to the sp^3-bonded {113} diamond surfaces – this structure is referred to as Type 2 diaphite [11]. HRTEM images of Type 2 diaphite from Canyon Diablo (Fig. 5a) and Popigai (Fig. 5b) samples are characterized by <121>
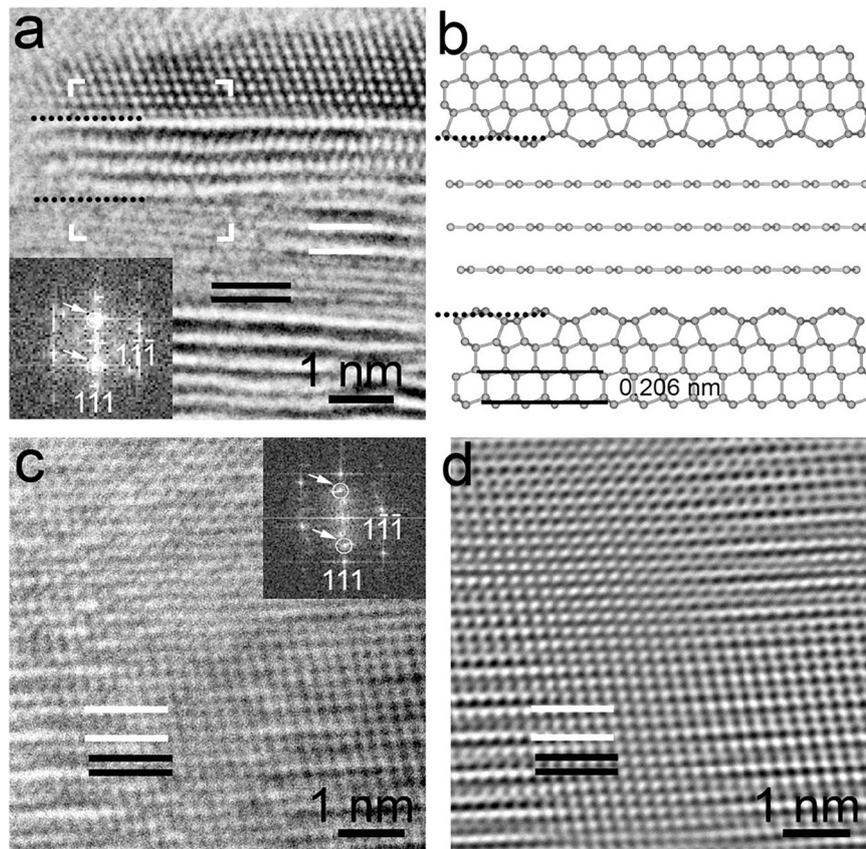
Fig. 4. Type 1 diaphite nanocomposites from impact diamonds. (a) HRTEM image of a graphene-diamond particle from the shocked Gujba meteorite (original image reported in [1]). White and black lines mark crystallographically related ∼0.34 nm {000l} graphite and ∼0.21 nm Å {111} diamond spacings, respectively. The FFT calculated from the TEM image shows the characteristic graphene (marked by white circles) and ⟨011⟩ diamond reflections. (b) DFT-calculated structure model of Type 1 diaphite for the area marked by white corners of (a). (c) Interfingering graphene-diamond nanocomposite structure observed within a Popigai diamond and its FFT with the characteristic graphene (marked by white circles) and ⟨011⟩ diamond reflections. (d) Background-filtered image of (c). Figures a, b, c, d were reported in [11] and were adapted with permission from American Chemical Society. Further permission related to the material excerpted should be directed to the ACS

diamond domains and subnanometer-sized regions containing ∼0.21 nm fringes arranged in a hexagonal pattern. We note that Fig. 5a has been previously interpreted as 2- and 4-layer thick {113} diamond twins. However, our DFT-based structure model (Fig. 5c) shows that such images are in fact consistent with Type 2 diaphite. The simulated HRTEM images based on the DFT model (Fig. 5c) indicate that these nanostructures correspond to a nanocomposite material consisting of sp^2- and sp^3-bonded carbon regions and the observation (Fig. 5d) matches with the DFT structure-based simulation (Fig. 5e).

Polysomatic series of diaphites and their advanced mechanical and optical properties

The diaphite nanotstructures comprise regions of diamond, graphitic carbon and interfaces between the two [11, 12]. In both Type 1 and Type 2 diaphite structures, the structural models can be constructed with varying amounts of these different diamond, graphene and interface regions. This is achieved by varying the size and compositing of the model cell in a systematic way. From this instance, the diaphite structures can be considered to form a polysomatic series. Such a consideration provides a framework for classifying the members of diaphites that are found in nature.

DFT calculation show that diaphites exist at relatively low energy and are competitive with graphite and diamond, i.e., they are readily achievable by laboratory scale methods and expected to be kinetically stable [11]. Diaphites are therefore candidates for obtaining metastable carbon materials formed by static or dynamic compression that are recoverable to ambient conditions. The diaphite nanostructures can be encountered during the compression phase or the rarefaction wave associated with shock impact and their occurrence could aid toward understanding the formation conditions and history of meteorites. According to a recent study diaphite-structured nanocarbons are widespread in nanodiamonds and their presence is responsible for unusual and previously unexplained features of their Raman and electron-energy loss spectra [14].

We predict that incorporation of these diaphite nanostructures into the sp^3-bonded diamond matrix will result in
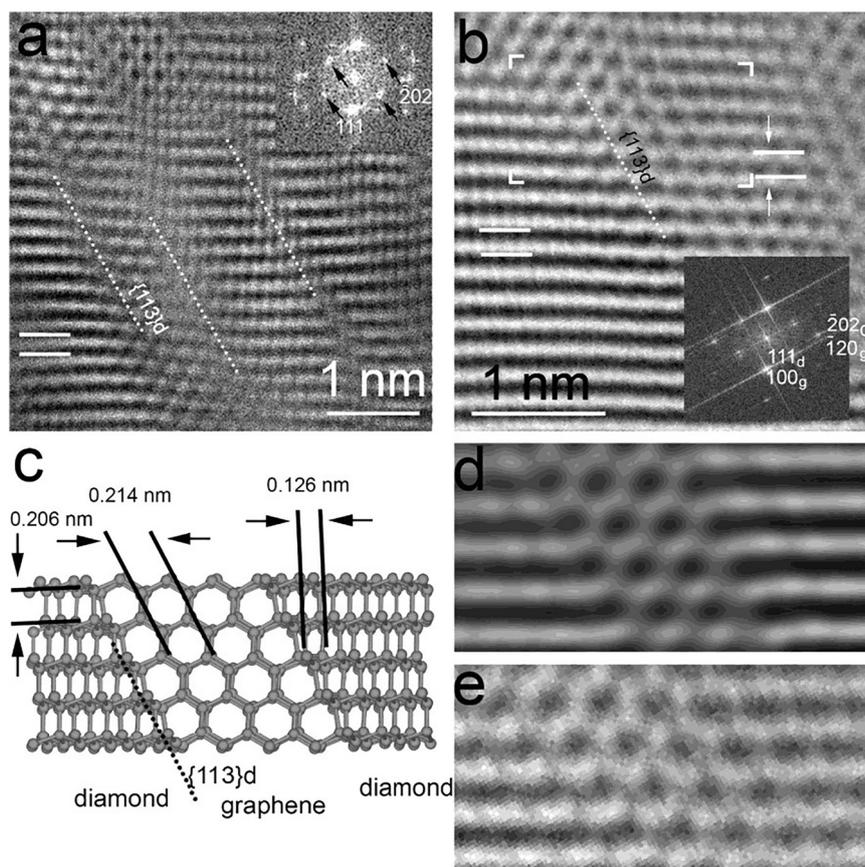
Fig. 5. Type 2 diaphite nanocomposites containing planar graphitic layers inserted at high angles within {113} diamond. a) Background-filtered uHRTEM image from Canyon Diablo meteorite with perpendicular 0.206 and 0.126 nm as well as hexagonally arranged 0.214 nm fringes (raw image reported in [4], copyright Springer Nature Ltd.). On the FFT the hexagonally arranged reflections are marked by black arrows. These hexagonal features were previously attributed to {113} diamond twins. b) Background filtered image uHRTEM image from Popigai with hexagonal features and their explanation with Type 2 diaphite intergrowth. (c) Structure model of Type 2 diaphite and its characteristic d spacings obtained from DFT calculations. (d) Simulated HRTEM image (upper panel) calculated from the structure shown in c) using the experimental microscopy conditions successfully reproduces the image contrast of the observed features (e) from the area marked by white corners of (b). The original images of b), c), d) and e) were reported in [11] and were adapted with permission from American Chemical Society. Further permission related to the material excerpted should be directed to the ACS

unusual effects on the mechanical, optoelectronic and thermoelectric properties [11, 12, 15]. For example, diamond is predicted to have a very high tensile strength, but it undergoes brittle fracture due to defects and the cleavage planes in its crystalline lattice. However, the graphitic layers within the diaphite structures will absorb the energy of a propagating crack resulting in fracture toughened ceramic behaviour [15]. Next, the graphitic to graphene-like structures will provide conducting nanodomains resulting in absorption of visible light. They will also disturb phonon propagation in the material thus lowering the thermal conductivity and perhaps leading to thermoelectric effects.

CONCLUSIONS

In summary, state-of-the-art TEM images reveal two new types of carbon nanostructures in natural impact diamonds and laboratory shocked samples. DFT calculations have shown that these correspond to Type 1 and Type 2 diaphite structures, containing graphitic and diamond layers joined at a well-defined interface. The energies of these diaphites are compatible with those of diamond and graphite polymorphs and they can readily be achieved during natural impact or laboratory shock compression conditions. Their presence is expected to significantly affect the properties of diamond-related materials.

ACKNOWLEDGEMENTS

REFERENCES

1. Garvie, L. A. J.; Németh, P.; Buseck, P. R. Transformation of graphite to diamond via a topotactic mechanism. *Am. Mineral.* **2014**, *99*(2–3), 531–8; https://doi.org/10.2138/am.2014.4658.

2. Németh, P.; Garvie, L. A. J. Extraterrestrial, shock-formed, cage-like nanostructured carbonaceous materials. *Am. Mineral.* **2020**, *105*(2), 276–81; https://doi.org/10.2138/am-2020-7305.

3. Frondel, C.; Marvin, U. B. Lonsdaleite, a hexagonal polymorph of diamond. *Nature* **1967**, *214*, 587–9; https://doi.org/10.1038/214587a0.

4. Németh, P.; Garvie, L. A. J.; Aoki, T.; Dubrovinskaia, N.; Dubrovinsky, L.; Buseck, P. R. Lonsdaleite is faulted and twinned cubic diamond and does not exist as a discrete material. *Nat. Commun.* **2014**, *5*, 6447. https://doi.org/10.1038/ncomms6447.

5. Németh, P.; Garvie, L. A. J.; Buseck, P. R. Twinning of cubic diamond explains reported nanodiamond polymorphs. *Sci. Rep.* **2016**, *5*, 18381; https://doi.org/10.1038/srep18381.

6. Salzmann, C. G.; Murray, B. J.; Shephard, J. J. Extent of stacking disorder in diamond. *Diamond Relat. Mater.* **2015**, *59*, 69–72; https://doi.org/10.1016/j.diamond.2015.09.007.

7. Murri, M.; Smith, R. L.; McColl, K.; Hart, M.; Alvaro, M.; Jones, A. P.; Németh, P.; Salzmann, C. G.; Corà, F.; Domeneghetti, M. C.; Nestola, F.; Sobolev, N. V.; Vishnevsky, S. A.; Logvinova, A. M.; McMillan, P. F. Quantifying hexagonal stacking in diamond. *Sci. Rep.* **2019**, *9*, 10334. https://doi.org/10.1038/s41598-019-46556-3.

8. Chu, P. K.; Li, L. Characterization of amorphous and nanocrystalline carbon films. *Mater. Chem. Phys.* **2006**, *96*(2–3), 253–77; https://doi.org/10.1016/j.matchemphys.2005.07.048.

9. Ohnishi, H.; Nasu, K. Generation and growth of sp3-bonded domains by visible photon irradiation of graphite. *Phys. Rev. B: Condens. Matter Mater. Phys.* **2009**, *80*, 014112; https://doi.org/10.1103/PhysRevB.80.014112.

10. Ferrari, A.; Basko, D. Raman spectroscopy as a versatile tool for studying the properties of graphene. *Nat. Nanotech.* **2013**, *8*, 235–46; https://doi.org/10.1038/nnano.2013.46.

11. Németh, P.; McColl, K.; Smith, R. L.; Murri, M.; Garvie, L. A. J.; Alvaro, M.; Pécz, B.; Jones, A. P.; Corà, F.; Salzmann, C. G.; McMillan, P. F. Diamond-graphene composite nanostructures. *Nano Lett.* **2020**, *5*, 3611–9. https://doi.org/10.1021/acs.nanolett.0c00556.

12. Németh, P.; McColl, K.; Garvie, L. A. J.; Salzmann, C. G.; Murri, M.; McMillan, P. F. Complex nanostructures in diamond. *Nat. Mater.* **2020**, *19*(11), 1126–31. https://doi.org/10.1038/s41563-020-0759-8.

13. Isobe, F.; Ohfuji, H.; Sumiya, H.; Irifune, T. Nanolayered diamond sintered compact obtained by direct conversion from highly oriented graphite under high pressure and high temperature. *J. Nanomater.* **2013**, 380165; https://doi.org/10.1155/2013/380165.

14. Németh, P.; McColl, K.; Garvie, L. A. J.; Salzmann, C. G.; Pickard, C. J.; Corà, F.; Smith, R. L.; Mezouar, M.; Howard, C. A.; McMillan, P. F. Diaphite-structured nanodiamonds with with six- and twelvefold symmetries. *Diam. Relat. Mater.* **2021**, *119*, 108573. https://doi.org/10.1016/j.diamond.2021.108573.

15. Zhang, S.; Zhang, Q.; Liu, Z.; Legut, D.; Germann, T. C.; Veprek, S.; Zhang, H.; Zhang, R. Ultrastrong p-bonded interface as ductile plastic flow channel in nanostructured diamond. *ACS Appl. Mater. Inter.* **2020**, *12*(3), 4135–42. https://doi.org/10.1021/acsami.9b19725.